JOINT EUROPEAN TORUS

JET–P(86)38

J.G. Cordey, M. Keilhacker
and M.L. Watkins

Prospects for Alpha Particle Heating in JET in the Hot Ion Regime

Prospects for Alpha Particle Heating in JET in the Hot Ion Regime

J.G. Cordey, M. Keilhacker
and M.L. Watkins

JET-Joint Undertaking, Culham Science Centre, OX14 3DB, Abingdon, UK

Preprint of Paper to be submitted for publication in
Physica Scripta

PROSPECTS FOR ALPHA PARTICLE HEATING IN JET IN THE HOT ION REGIME

J G Cordey, M Keilhacker, M L Watkins

JET Joint Undertaking, Abingdon, Oxon OX14 3EA, England.

Abstract

The prospects for alpha particle heating in JET are discussed. A computational model is developed to represent adequately the neutron yield from JET plasmas heated by neutral beam injection. This neutral beam model, augmented by a simple plasma model, is then used to determine the neutron yields and fusion Q-values anticipated for different heating schemes in future operation of JET with tritium. The relative importance of beam-thermal and thermal-thermal reactions is pointed out and the dependence of the results on, for example, plasma density, temperature, energy confinement and purity is shown. Full 1½-D transport code calculations, based on models developed for ohmic, ICRF and NBI heated JET discharges, are used also to provide a power scan for JET operation in tritium in the low density, high ion temperature regime. The results are shown to be in good agreement with the estimates made using the simple plasma model and indicate that, based on present knowledge, a fusion Q-value in the plasma centre above unity should be achieved in JET.

1. INTRODUCTION

The performance of JET will be determined to a large extent by the thermal transport properties and purity of the JET plasma under conditions of strong additional heating power. To approach ignition in JET will require energy confinement times, τ_ε, of about 1-2s and an effective ionic charge, Z_{eff}, close to unity. At present the confinement time in JET ohmic discharges is ~ 0.8s and this is reduced to $\lesssim$ 0.4s in the presence of strong additional heating (see, for example Figure 1). The lowest values of Z_{eff} presently obtained are in the range 2 - 2.5 (Figure 2). As a result progress towards ignition, as represented in the $n_i(o)\ \tau_\varepsilon$ versus $T_i(o)$ space (Figure 3, where $n_i(o)$ and $T_i(o)$ are respectively the central values of the ion density and temperature and τ_ε is the global energy confinement time), is on a broad front with similar values of the product $n_i(o)\ \tau_\varepsilon\ T_i(o)$ being obtained in high density, low temperature, ohmic plasmas and in low density, high temperature plasmas with strong additional heating (8 MW of neutral deuterium injection at 75 kV and/or $\lesssim$ 6 MW of ion cyclotron resonance heating).

In the present paper we review the approach to ignition in JET, concentrating on the low density, high temperature ("hot ion") regime. It was recognised already in the JET design document R5[1] that in an approach to ignition in the central plasma ("core ignition") a significant fraction of the reactivity would come from reactions between the injected beam ions and the background thermal ions. The additional α-particles produced by these beam-thermal reactions were seen as an extra heating source enabling core ignition to be obtained with lower additional heating power. Calculations were also made of the fusion Q (= fusion energy release/input power) as a function of the plasma density and confinement time for the operation of JET as a hot ion driven system. Recent experiments on JET have enabled a more precise assessment of its potential to operate in this regime.

The paper is organized as follows. In Section 2 the scaling of the fusion Q-value with plasma parameters for neutral beam injection is examined. In Section 3, the neutron yields and fusion Q-values obtained in present JET experiments in deuterium are compared with the expectations of neutral beam theory. In Section 4, this neutral beam model is augmented by a simple plasma model in order to extrapolate to higher power operation in JET with tritium and to determine the deuterium-tritium fusion Q-values to be expected. Finally, in Section 5, full 1½-D transport code calculations based on models developed for various JET plasmas are used to demonstrate that the Q-values thus obtained are similar to those obtained using the simpler plasma models.

2. THE SCALING OF THE FUSION Q-VALUE WITH PLASMA PARAMETERS FOR NEUTRAL BEAM INJECTION

The most general scenario is the injection of counterstreaming deuterium and tritium beams into a D-T plasma. In this case there are three sources of fusion reactions, beam-beam, beam-thermal and thermal-thermal reactions. In the present paper, we consider only the contributions of the latter two sources to the fusion Q, which can be obtained from the thermal and fast ion distribution functions and may be put in the form:

$$Q = \underbrace{\frac{n_D n_T \overline{\sigma v}_{th}(T_i)\, Y}{P}}_{\text{thermal-thermal}} + \underbrace{\frac{C_1 T_e^{\frac{3}{2}} Y}{n_e E_D} n_T \overline{\sigma v}_D(E_D/T_e)}_{\text{beam-thermal}}$$

where n_e, n_D, n_T are the electron and background deuterium and tritium densities, T_e and T_i are the electron and ion temperatures, P is the total external neutral beam injection power at an energy, E_D, Y is the fusion yield, $\overline{\sigma v}_{th}$ and $\overline{\sigma v}_D$ are fusion reaction rate coefficients and C_1 is a constant.

Of major importance is the dependence of each term in the above equation on the density: at very high densities ($>10^{20}m^{-3}$) the thermal-thermal term is dominant and we have the conventional reactor operation; at moderate densities ($2-4 \times 10^{19}$ m^{-3}) the beam-thermal fusion term becomes dominant and this is the two-component tokamak (TCT) type of operation discussed originally by Dawson, Furth and Tenney[2]. At low densities ($<2x10^{19}m^{-3}$) it would be necessary to consider also the beam-beam fusion term. The colliding beam tokamak [3,4], in which counter-streaming deuterium and tritium beams are injected to maximise the number of "head-on" fusion reactions, is a good example of how beam-beam fusion may be exploited.

Of importance also is the dependence of each term in the above equation on the impurity concentration: the thermal-thermal term is quite strongly affected through the reduction of the product $n_D n_T$ by the dilution effect of the impurities; the beam-thermal term is less affected by dilution since it depends only linearly on n_T. The beam-beam contribution would be completely unaffected by impurity dilution but the angular scattering of the injected fast ions is proportional to Z_{eff} and so the reactivity from "head-on" collisions would be reduced.

3. NEUTRON YIELDS IN PRESENT JET EXPERIMENTS

In a recent series of experiments up to 8 MW of 75 kV deuterons have been injected into deuterium plasmas with currents in the range I = 1 - 5 MA and a standard JET geometry with an elongation K = 1.45. A further 6 MW of ICRH was also added making a total input power of up to 16 MW, including the ohmic heating contribution. The neutron yields are shown as a function of density in Figure 4, and indicate as expected a maximum at low line - averaged electron densities, $\bar{n} \sim 2\text{-}3 \times 10^{19} m^{-3}$. The resulting fusion Q-values in deuterium are shown as a function of density in Figure 5. The discharges with the largest Q-values ($Q_{DD} \sim 2.5 \times 10^{-4}$, which corresponds to $Q_{DT} \sim 0.2$ for deuterium injection into a tritium plasma) had current in the range 2 - 3 MA and were located on the inside wall or had an X-point. Their confinement times were about 0.3s. At first sight it would appear from Figure 5 that combined heating (NBI and ICRH) gives a lower Q-value than NBI alone. However, this maybe because combined heating experiments have not yet been performed in the X-point configuration.

These experimental Q-values are reasonably reproduced by a theoretical model for the attenuation of the neutral beam and the subsequent slowing down of the fast ions. This model uses the neutral beam injection geometry, measured neutral beam energy, power and species mix and the measured electron and ion temperatures and electron density in the actual plasma geometry of JET. The flux surfaces are obtained from the best fit to the magnetic measurements made on the vacuum wall of a set of solutions to the Grad-Shafranov equilibrium equation containing two variable parameters describing the current profile [5]. This equilibrium is subsequently parameterised in line with the "moments approach" [6], in which the "radial" co-ordinate, ρ, is the horizontal half-width of a flux surface normalised to that at the limiter, ρ_a. The radial electron temperature profile is obtained from the electron cyclotron emission [7] at the second harmonic. The central ion temperature is obtained from a crystal spectrometer measurement[8] of a Ni^{26+} line, which is routinely available during neutral beam injection, but which slightly overestimates the background ion temperature for intense neutral beam injection. The ion temperature profile is taken to be the same as that of the electrons. The line-averaged density is measured by a single-channel microwave interferometer [9] viewing along a vertical chord near the plasma centre (major radius, R=3.14 m). The density profile is obtained from the seven channel far infrared interferometer, by fitting the data to a functional form, $n_e = n_e(o)(1-\rho^2)^\gamma + n_a$. Z_{eff} is determined from the visible bremsstrahlung viewing along a single vertical chord (R=3.14 m). Its profile is assumed to be flat and, for the present results, is assumed to comprise a mixture of deuterium, oxygen and carbon, with three times the concentration of carbon as oxygen. The assumed plasma geometry and profiles for JET Pulse Number 7958 are shown in Figure 6.

For the specified plasma geometry and profiles, the birth profile of fast ions is calculated using a multiple pencil beam model in which many filamentary neutral currents are attenuated by electron impact ionisation, proton ionisation and charge-exchange, including capture by impurities. A time-dependent solution to the Fokker Planck equation, representing the slowing down of fast ions, provides the neutron yields that arise from beam-thermal interactions together with the corresponding fusion Q-values in deuterium and the equivalent fusion Q-values assuming deuterium injection into a 100% tritium plasma.

In Figure 7, we show as a function of time for Pulse Number 7958 the total neutral injection power (8 MW of deuterium injection at 75 kV with an assumed power species mix of 74%: 16%: 10%); the neutron yields determined from the neutron flux measurements [10]; the neutron yields calculated by the neutral beam physics model and the thermal plasma parameters; the resultant beam-plasma fusion Q-values for deuterium injection into a deuterium plasma and also into a tritium plasma. It is to be noted that the time variation of the measured and calculated neutron yields are in very good agreement. The measured total neutron yield is some 30% lower than that calculated, indicating possible errors in the assumed plasma parameters (particularly, the ion temperature and the effective ionic charge) or in the neutral beam physics model. None-the-less for the present considerations this degree of accuracy is acceptable.

4. EXTRAPOLATION TO FUSION CONDITIONS

We now turn to the significance of the above for the production of α-particles in JET.

A simple plasma model is assumed with density and temperature profiles of the forms, $n_e = n_e(0)(1-\rho^2)^{0.5}$ and $T_e = T_e(0)(1-\rho^{1.5})$ taken from a 3 MA JET pulse with an elongation of 1.45 and $\rho_a = 1.17$m. For given volume-averaged electron density, $\bar{n}_e = \int n_e dV / \int dV$, energy confinement time, τ_ε , and external input power, P, the central temperatures are obtained from a simple global energy balance equation,

$$P = \frac{3\int n_e[T_e + (n_i + n_o + n_c)\frac{T_i}{n_e}]dV}{2\tau_\varepsilon}$$

The ion and electron temperatures are assumed to be related by a simple equipartition formula $T_i = 2T_e/(1+\bar{n}_e^2 10^{-40})$. The deuterium-tritium (n_i), oxygen (n_o) and carbon concentrations (n_c) are obtained by specifying Z_{eff} and assuming $n_c = 3n_o$. The external power is assumed to comprise of a combination of up to 40 MW of neutral deuterium injection at 160 kV (assuming a power species mix of 63%:29%:8%) and up to 20 MW of ICRF.

4.1 Neutral Beam Injection at a total power level of 20 MW

We consider in the first instance the particular case of 20 MW of 160 kV deuterium injection into a 50:50 D-T mixture. In Figure 8 the global Q-value is shown versus density for four different values of τ_ε = 0.4, 0.8, 1.2 and 1.6s. The lower τ_ε is typical of L-mode behaviour in JET, where τ_ε is only weakly dependent on density and increases with current in the range $\tau_\varepsilon \sim 0.1 - 0.4$s. The intermediate value (τ_ε = 0.8s) is typical of present ohmic plasmas and presumably would be reached with H-mode behaviour in JET. The highest values ($\tau_\varepsilon \sim 1.2$-1.6s) are those required to approach ignition in JET and, for a power level of 20 MW, correspond to plasmas close to the β limits of 3% ($\tau_\varepsilon \sim 1.3$s) and 4.8% ($\tau_\varepsilon \sim 2$s) expected, respectively, for 4MA X-point and 7 MA limiter operation in JET. The relative importance of the thermal-thermal and beam-thermal contributions to the total Q-value is also shown.

From these curves the following observations can be made:

First, the maximum Q-value is obtained at relatively low densities, $\bar{n}_e = 2 - 3 \times 10^{19}$ m^{-3} for the lower values of τ_ε and only slightly higher $\bar{n}_e = 4 - 6 \times 10^{19}$ m^{-3} for the higher values of τ_ε. This arises from the need to keep the plasma temperature sufficiently high and near the optimum value (~ 12-15 keV) as the density is varied.

Second, for τ_ε up to 0.4s the beam-thermal fusion term is dominant for the entire density range, and it is only for confinement times greater than 0.8s that the thermal-thermal fusion term becomes significant.

The Q-values are reduced, of course, with increasing impurity concentration, as shown in Figure 9 for the same conditions as in Figure 8 but with Z_{eff} = 3.

4.2 Combined Neutral Beam and ICRF Heating, Each at a Power Level of 20 MW

The same curves as in Figure 8 may be used to assess the prospects of a combined heating scenario in which 20 MW of ICRH is added to the 20 MW of NBI (Figure 10). In this case, since the total input power has been doubled, both the value of τ_ε used to label each curve and the magnitude of the Q-value obtained have to be reduced to one-half of their original values. Also plotted on Figure 10 ,are the conditions of constant electron temperature, from which it is seen that, as the density increases, the maximum gain in the Q-value is obtained by increasing τ_ε such that the central electron temperature is maintained at approximately 15 keV.

4.3 Central Q-Values

In the central part of the discharge (defined as the inner quarter volume, or roughly, the region within q = 1) the Q-values (referred to as $Q_{1/4}$) are rather larger, as shown in Figure 11 for NBI alone and Figure 12 for the combined heating scheme with the ICRH assumed to be deposited within the inner quarter volume. For fixed confinement time and at the lowest densities, when the beam-thermal interactions dominate, $Q_{1/4}$ is lower with combined heating, while at the higher densities, $Q_{1/4}$ is higher with the combined heating, with the higher temperatures more than compensating for the increased heating power.

It should be noted that to obtain $Q_{1/4} \gtrsim 2.5$ requires $\tau_\varepsilon \gtrsim 0.8$s and the difference between Q and $Q_{1/4}$ is less with combined heating because of the assumption that the ICRF is deposited wholly within the inner quarter volume.

4.4 Dependence of Q-Values on the level of Neutral Injection Power

As shown by the power scan with NBI alone at the fixed density, $\bar{n}_e = 4 \times 10^{19}\ m^{-3}$ (Figure 13), a substantial increase in the beam power to about 40 MW would be necessary in order to achieve $Q \gtrsim 1$ for $\tau_\varepsilon \gtrsim 0.4$ s or $Q \gtrsim 2.5$ for $\tau_\varepsilon \gtrsim 0.8$s. Taking account of the α-power in addition to the external input power might even lead to core ignition at lower external power levels and at somewhat higher densities, $\bar{n}_e \gtrsim 8 \times 10^{19}\ m^{-3}$ (Figure 14).

5. FULL TRANSPORT CODE SIMULATIONS OF THE HOT ION REGIME

Plasma transport models used in a full 1½-D transport code [11] have been developed for various JET plasmas, including ohmic [12], ICRF [13] and NBI [14]. In particular, low density, high temperature plasmas with neutral beam injection were examined in [14] and found to be well simulated using an anomalous electron thermal diffusivity of the ALCATOR-INTOR or Coppi-Mazzucato-Gruber form ($\chi_{eAI} = 5.10^{19} n_e^{-1}$ or $\chi_{eCMG} = 3.10^{15} a B_T n_e^{-0.8} (RqT_e)^{-1} A_p^{-0.5}$); ion thermal diffusivity of the Chang and Hinton form with an anomaly factor, $\alpha_i = 4$; anomalous diffusive and convective particle fluxes; oxygen/carbon and nickel impurities; neoclassical resistivity; classical energy transfer between electrons and ions; and the Kadomtsev reconnection model for sawteeth. Confinement degradation during NBI was simulated by increasing, outside the q = 1 region, the electron thermal diffusivity for ohmic plasmas by either a fixed factor, $\alpha_e \lesssim 2$, or a power-dependent factor, $\alpha_{ep} = \int_0^V P_{total,e} dV / \int_0^V P_{OH} dV$.

Using the model with χ_{eCMG} and α_{ep}, a series of calculations has been performed for various power levels (in the range 5-40 MW) of neutral deuterium injection at 160 kV into a deuterium-tritium plasma assumed to be maintained at a 50-50 mixture. The density increase during neutral beam injection is limited by pumping 10% of the edge outflux. This maintains the volume-averaged electron density within the range 2-4 x 10^{19} m^{-3} and Z_{eff} in the range 2-3. The global energy confinement time is calculated to be approximately 0.4s irrespective of the level of additional heating power. The Q-values obtained in these calculations are plotted in Figure 15, which shows also that the results of the simple plasma model for $\bar{n}_e = 2 \times 10^{19}$ m^{-3} and $Z_{eff} = 1$ and $\bar{n}_e = 4 \times 10^{19}$ m^{-3} and $Z_{eff} = 3$ cover the range of Q-values obtained from the transport code calculations.

6. SUMMARY

We have shown that we have been able to reproduce fairly accurately the present JET experimental data for neutron yields using the appropriate plasma conditions and a neutral beam deposition and slowing down model. This gives confidence in extrapolating to JET operation in tritium, and the level of alpha particle heating which might be expected for different plasma conditions and heating powers has been determined. Concentrating on the low-density, hot ion mode of operation, central Q-values in excess of 1.0 could be expected for confinement times in excess of 0.4s. However, low Z impurities can reduce considerably the Q-values.

Further gains in these Q-values would require improved plasma confinement, a substantial increase in the neutral injection power or beneficial synergistic effects between the NBI and ICRH. Improved plasma confinement might be found in the central plasma or achieved through X-point operation in JET, leading to central Q-values in excess of 2.5 and global Q-values in excess of 1 for confinement times in excess of 0.8s. If the confinement time were considerably less than 0.4s, then it might be preferable to inject deuterium beams into a low-density, 100% tritium plasma, thereby increasing by a factor of two the beam-thermal contribution at the expense of the thermal-thermal contribution. Leaving aside the technical difficulties involved in the production of a tritium beam, additional gains are to be expected with balanced injection of both deuterium and tritium beams into a 50:50 D-T plasma for which there are two clear advantages: first, at low density and τ_ε the beam-beam contribution would become very significant; second, the tritium beam would give better control over the D-T background mixture. With combined NBI and ICRH, higher Q-values might result from using the ICRF to 'clamp' the injected particles at the optimum energy for fusion. There are of course several problems to be overcome with this scheme, the main one being to ensure that most of the ICRH power is actually absorbed in the injected deuterons rather than on electrons, background deuterons or on a minority hydrogen component of the background plasma as is the case in some of the present JET plasmas with second harmonic deuterium heating.

ACKNOWLEDGEMENTS

The authors are indebted to members of the JET Experimental team for the data which has been presented or quoted and to Mrs P M Stubberfield, M Cox and D G Muir for development of the computational models.

REFERENCES

[1] The JET Project - Design Proposal, Report EUR5516e, Commission of the European Communities, Luxembourg, 1975.

[2] Dawson, J.M., Furth, H.P. and Tenney, F., Phys. Rev. Lett 26, 1156(1971).

[3] Jassby, D.L., Nucl. Fusion 16, 15(1976).

[4] Cordey, J.G. and Core, W.G., Nucl. Fusion 15, 710(1975).

[5] Blum, J., Le Foll, J. and Thooris, B., Comp. Phys. Comm. 24, 235(1981).

[6] Lao, L.L., Hirshman, S.P. and Wieland, R.M., Phys. Fluids 24, 1431(1981).

[7] Costley, A.E., et al., IV Int. Workshop on ECE and ECRH, Frascati, 1984, 1, ENEA, Rome, 1984.

[8] Källne, E., Private Communication, 1986 (To be published).

[9] Fessey, J.A., Gowers, C.W., Hugenholtz, C.A. and Slavin, K., JET Preprint, JET-P(85)04, 1985 (To be published in J. Phys. E (1986)).

[10] Jarvis, O.N., et al., JET Internal Report, JET-IR(84)02,1984.

[11] Watkins, M.L., et al., J. Nucl. Mater. 121, 429(1984).

[12] Behringer, K.H., et al., in Plasma Physics and Controlled Nuclear Fusion Research (Proc. 10th Int. Conf., London, 1984) 1, 291, IAEA, Vienna, 1985.

[13] Taroni, A., et al., Proc. 12th Eur. Conf. on Cont. Fusion and Plasma Physics, Budapest, 1985, 9F(I), 22, EPS, 1985.

[14] Watkins, M.L., Houlberg, W.A., Kupschus, P., Stubberfield, P.M. and Taroni, A., Proc. 13th Eur. Conf. on Cont. Fusion and Plasma Heating, Schliersee, 1986, 10C(I), 156, EPS, 1986.

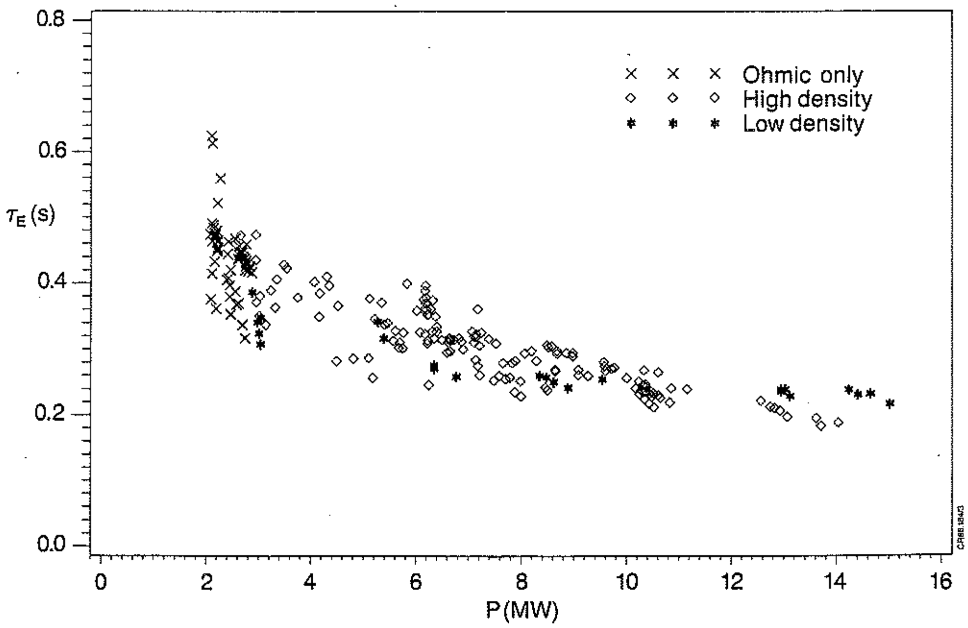

Fig. 1 Energy confinement time as a function of total input power (ohmic, NB and RF) for 3 MA JET discharges.

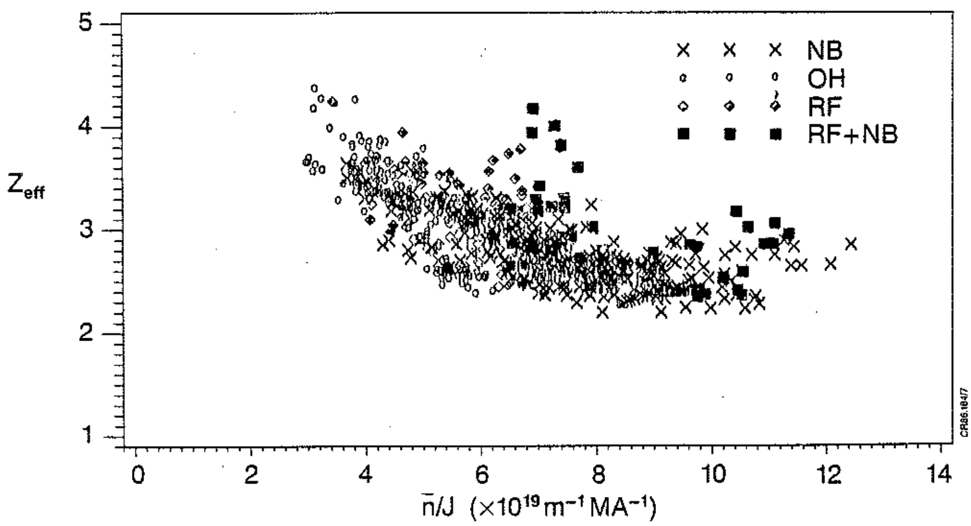

Fig. 2 Z_{eff} from the visible bremsstrahlung measurement as a function of the ratio of the line-averaged electron density to the mean current density for different heating combinations.

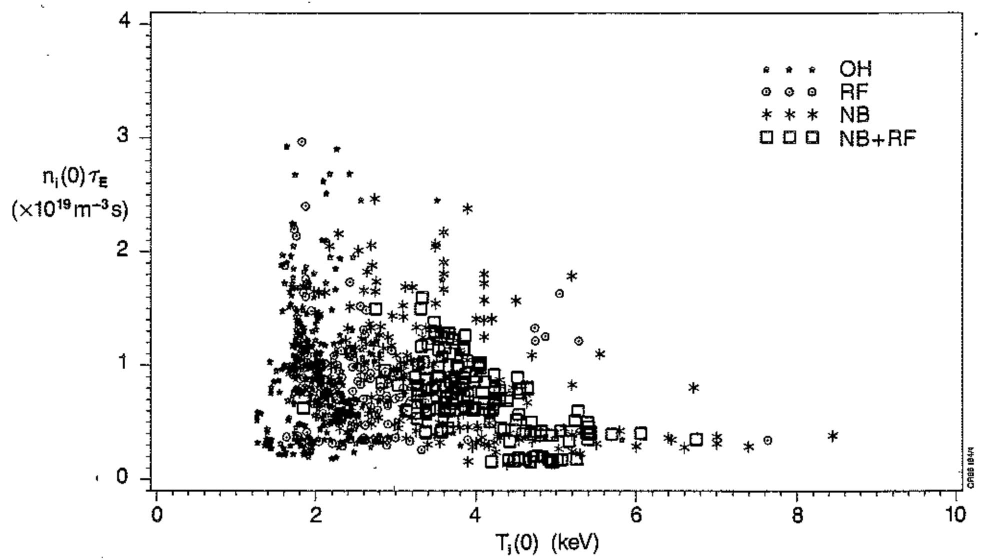

Fig. 3 The Lawson plot for discharges with different plasma densities, currents and heating combinations.

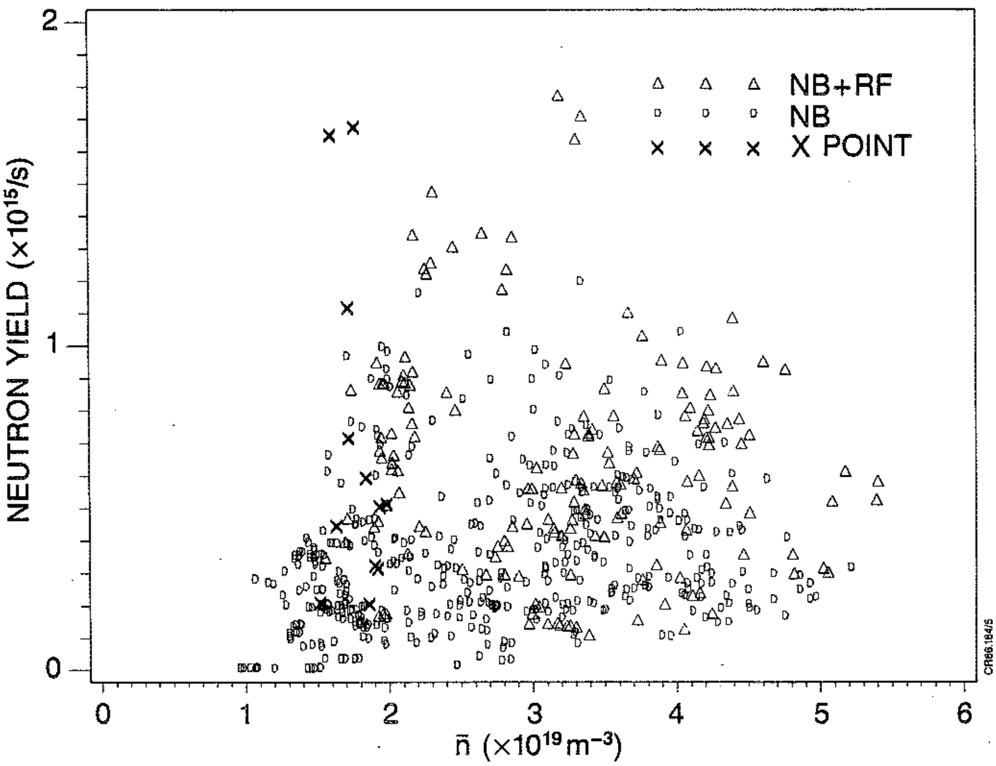

Fig. 4 Experimental neutron yields versus line-averaged electron density for different heating combinations in JET.

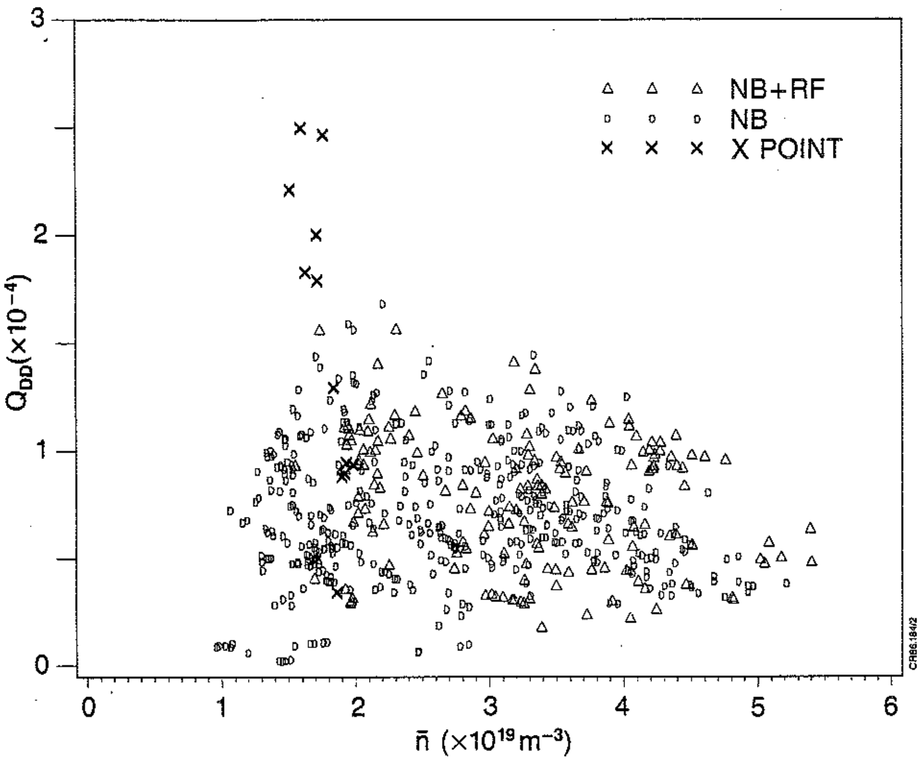

Fig. 5 Experimental Q_{DD} versus line-averaged electron density for different heating combinations in JET.

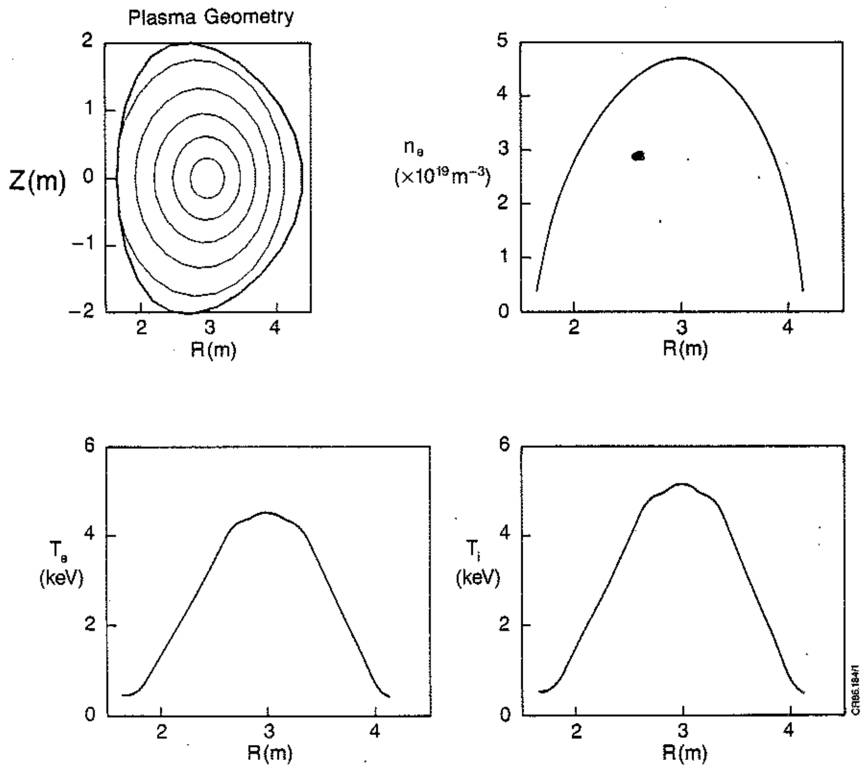

Fig. 6 Plasma geometry and profiles of electron density, electron temperature and ion temperature for JET Pulse Number 7958.

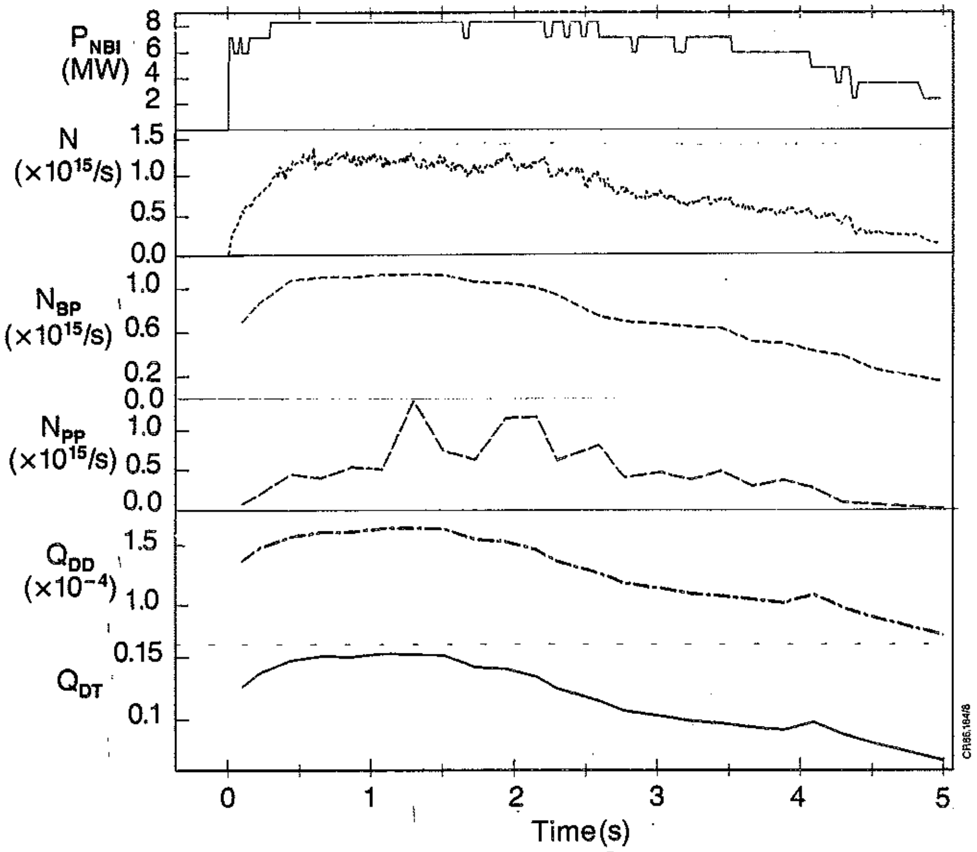

Fig. 7 The time variation in JET Pulse Number 7958 of the neutral beam injection power (75 kV deuterium injection), the measured neutron fluxes, the calculated beam-thermal neutron fluxes, the calculated thermal-thermal neutron fluxes, the calculated beam-thermal Q_{DD}, and the calculated beam-thermal Q_{DT} (assuming deuterium injection into a 100% tritium plasma).

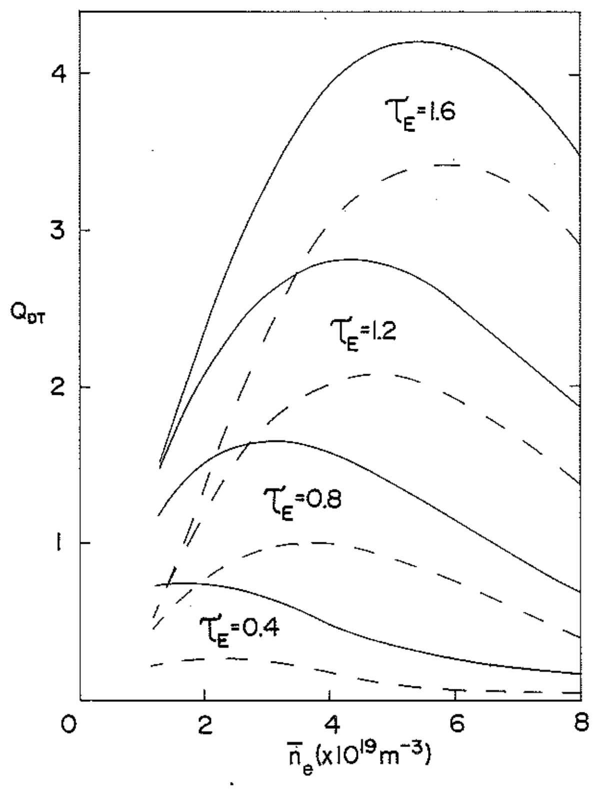

Fig. 8 Global Q_{DT} versus volume-averaged electron density at fixed values of τ_E for 160kV deuterium injection at a total power of 20MW and a 50:50 pure D-T plasma. The dotted lines are the thermal contribution.

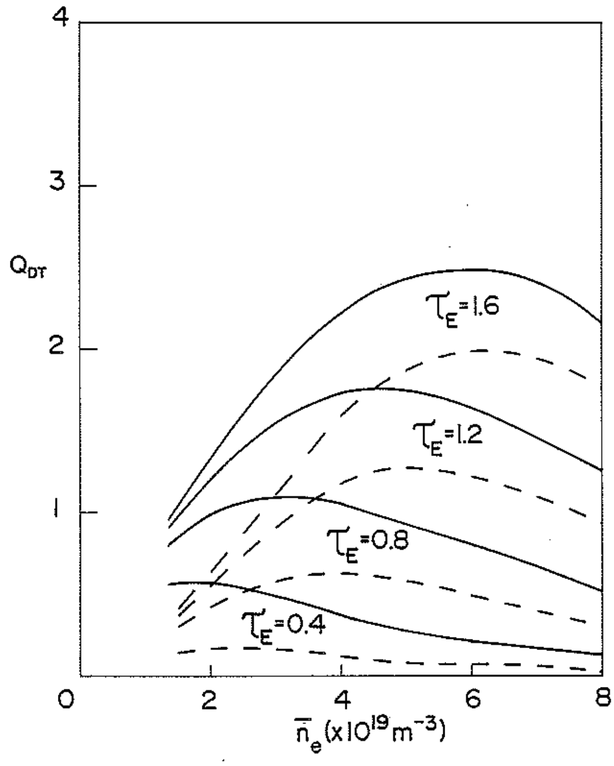

Fig. 9 Global Q_{DT} versus the volume-averaged electron density at fixed values of τ_E for 160kV deuterium injection at a total power of 20MW and a 50:50 D-T plasma with $Z_{eff}=3$. The dotted lines are the thermal contribution.

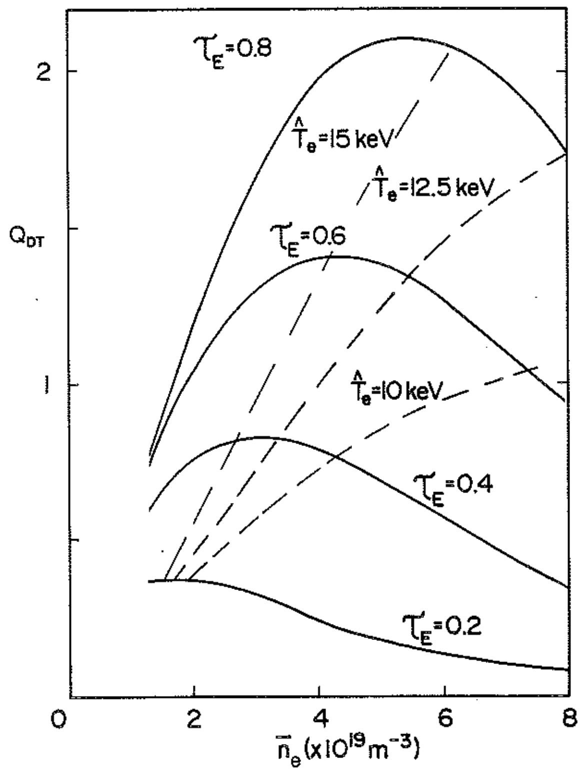

Fig. 10 Global Q_{DT} versus volume-averaged electron density at fixed values of τ_E for a total power of 20MW deuterium injection at 160kV and 20MW of RF and a 50:50 pure D-T plasma. The dotted lines are conditions of constant electron temperature.

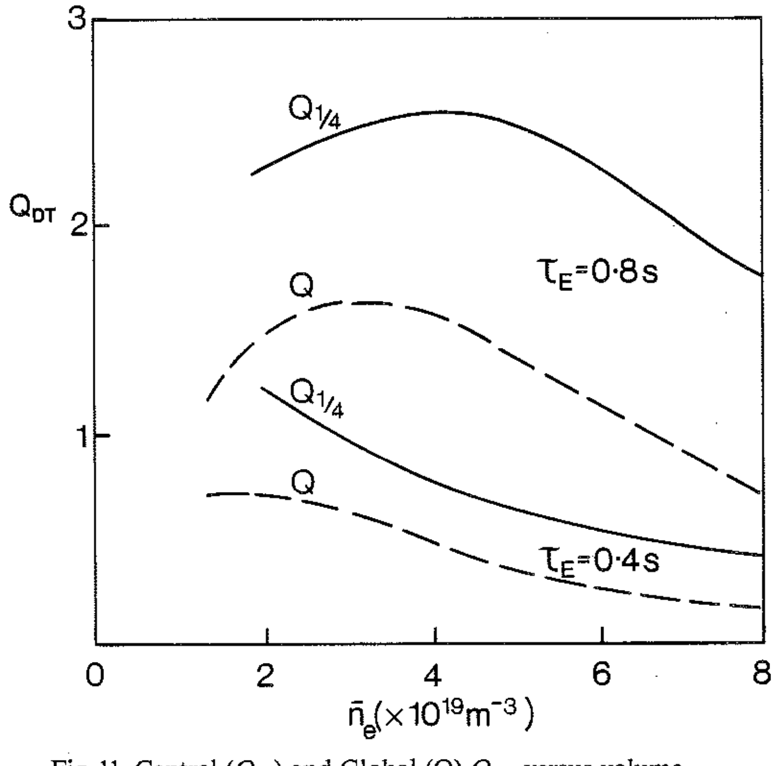

Fig. 11 Central ($Q_{1/4}$) and Global (Q) Q_{DT} versus volume-averaged electron density at fixed values of τ_E for 160kV deuterium injection at a total power of 20MW and a 50:50 pure D-T plasma.

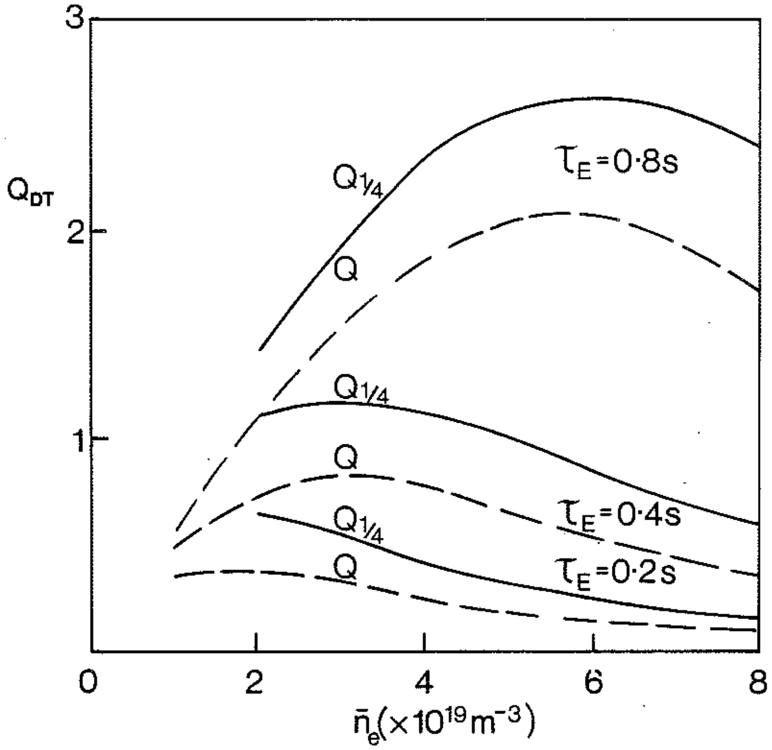

Fig. 12 Central ($Q_{1/4}$) and Global (Q) Q_{DT} versus volume-averaged electron density at fixed values of τ_E for 20MW deuterium injection at 160kV and 20MW of RF deposited centrally and a 50:50 pure D-T plasma.

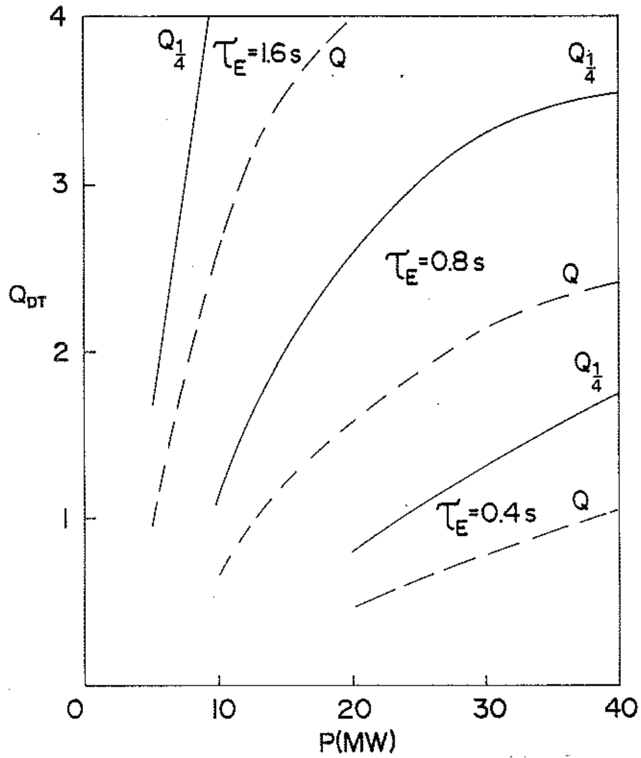

Fig. 13 Central ($Q_{1/4}$) and Global (Q) Q_{DT} versus deuterium neutral injection power at 160kV at fixed values of τ_E for a 50:50 pure D-T plasma at a volume-averaged electron density of $4\times10^{19}m^{-3}$.

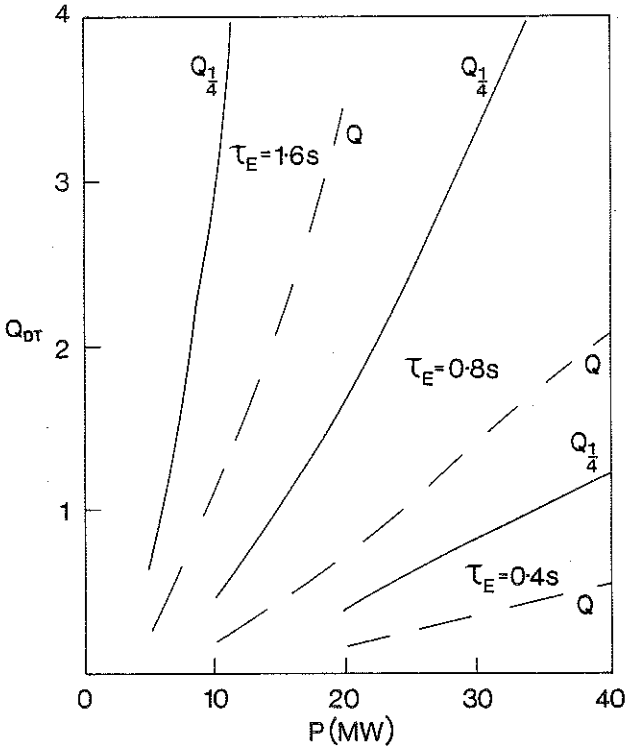

Fig. 14 Central ($Q_{1/4}$) and Global (Q) Q_{DT} versus deuterium neutral injection power at 160kV at fixed values of τ_E for a 50:50 pure D-T plasma at a volume-averaged electron density of $8\times10^{19}m^{-3}$.

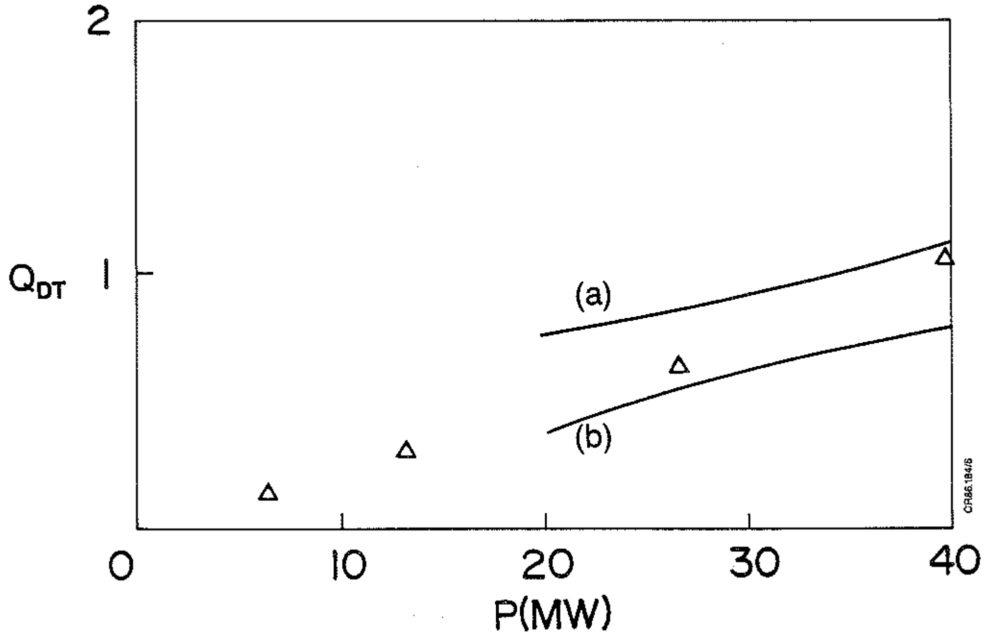

Fig. 15 Global Q_{DT} versus deuterium neutral injection power at 160kV for full 1½-D transport code calculations with a 50:50 D-T impure plasma. The results of the simple plasma model (a) for $\bar{n}_e=2\times10^{19}m^{-3}$ and $Z_{eff}=1$ and (b) for $\bar{n}_e=4\times10^{19}m^{-3}$ and $Z_{eff}=3$ are also shown.